EPJ B
Condensed Matter and Complex Systems
EPJ.org
your physics journal

Eur. Phys. J. B **84**, 265–271 (2011) DOI: 10.1140/epjb/e2011-20650-7

Hydrostatic pressure, impurity position and electric and magnetic field effects on the binding energy and photo-ionization cross section of a hydrogenic donor impurity in an InAs Pöschl-Teller quantum ring

M.G. Barseghyan, M.E. Mora-Ramos and C.A. Duque

EDP SCIENCES
Società Italiana di Fisica
Springer

Eur. Phys. J. B **84**, 265–271 (2011)
DOI: 10.1140/epjb/e2011-20650-7

THE EUROPEAN PHYSICAL JOURNAL B

Regular Article

Hydrostatic pressure, impurity position and electric and magnetic field effects on the binding energy and photo-ionization cross section of a hydrogenic donor impurity in an InAs Pöschl-Teller quantum ring

M.G. Barseghyan[1], M.E. Mora-Ramos[2], and C.A. Duque[3,a]

[1] Department of Solid State Physics, Yerevan State University, Al. Manookian 1, 0025 Yerevan, Armenia
[2] Facultad de Ciencias, Universidad Autónoma del Estado de Morelos, Ave. Universidad 1001, CP 62209, Cuernavaca, Morelos, Mexico
[3] Instituto de Física, Universidad de Antioquia, Calle 67 No. 53-108, A.A. 1226, Medellín, Colombia

Received 8 August 2011
Published online 10 November 2011 –

Abstract. Using the variational method and the effective mass and parabolic band approximations, the behaviour of the binding energy and photo-ionization cross section of a hydrogenic-like donor impurity in an InAs quantum ring, with Pöschl-Teller confinement potential along the axial direction, has been studied. In the investigation, the combined effects of hydrostatic pressure and electric and magnetic fields applied in the direction of growth have been taken into account. Parallel polarization of the incident radiation and several values of the applied electric and magnetic fields, hydrostatic pressure, and parameters of the Pöschl-Teller confinement potential were considered. The results obtained can be summarised as follows: (1) the influence of the applied electric and magnetic fields and the asymmetry degree of the Pöschl-Teller confinement potential on the donor binding energy is strongly dependent on the impurity position along the growth and radial directions of the quantum ring, (2) the binding energy is an increasing function of hydrostatic pressure and (3) the decrease (increase) in the binding energy with the electric and magnetic fields and parameters of the confinement potential (hydrostatic pressure) leads to a red shift (blue shift) of the maximum of the photo-ionization cross section spectrum of the on-centre impurity.

1 Introduction

Quantum dot (QD) and quantum ring (QR) semiconductor structures have been fabricated using self-assembly techniques, such as those shown in the experimental work of Petroff et al. [1]. Both QD and QR systems are the subject of great interest for their application in optoelectronic devices [2–5]. On the other hand, if one goes beyond the case of single nanostructures, the artificial molecules consisting of coupled QDs or QRs are particularly attractive because they show great promise for quantum information processing [6] and terahertz devices [7].

In a work published several years ago, Lorke et al. first observed a far-infrared optical response in self-assembled QRs, revealing a magneto-induced change in the ground state from angular momentum $l = 0$ to $l = -1$, with a flux quantum piercing the interior [8]. On the other hand, the study in recent years of the electronic properties of hydrogenic-like impurities in low-dimensional semiconductor heterostructures has become a research subject of great interest. This stems from the existence of vast possibilities associated with the purposeful manipulation of the impurity binding energy by means of external influences, and hence the possibility of controlling the electronic and optical properties of functional devices based on such heterostructures [9]. In contrast to the case of massive samples, in quantum heterostructures the effect of external influences such as hydrostatic pressure, external fields etc. on the impurity binding energy – as well as other features – , depends on the shape and size of sample, on the shape of the confinement potential energy, and also on the impurity centre position. In this sense, Barticevic et al. calculated the energy spectrum and optical absorption properties of QRs subject to magnetic fields [10]; although this study neglected the excitonic and impurity effects. Furthermore, a theoretical work on the shallow-donor states in toroidal GaAs-(Ga,Al)As QRs, with the use of the effective mass approximation together with a variational calculation, is presented in reference [11]. The work includes the effect of an axial magnetic field on free-electron and shallow-donor states.

An analytical approach to the problem of an electron impurity positioned in a QR in the presence of crossed axially-directed homogeneous magnetic and

[a] e-mail: cduque_echeverri@yahoo.es

radially-directed electric fields appears in the work by Monozon and Schmelcher [12]. In addition, Aichinger et al. [13] have considered the effects of impurities and changing ring geometry on the many electron's energy levels in a QR under the influence of an external magnetic field.

Theoretical studies about the photo-ionization cross section (PCS) in low dimensional semiconductor systems have been the subject of great interest as well. The reason for this is that the PCS provides useful information that helps our understanding of the optical properties of confined carriers. It also characterises the impurity states in the heterostructure. Among the different parameters to be considered in the calculation of the PCS, we can mention: (1) the confinement degree [14,15]; (2) the energy and polarization of the incident photon [16]; (3) the shape and geometrical dimensions of the heterostructures [17]; (4) the presence of applied electric and/or magnetic fields [18–20], and (5) hydrostatic pressure and temperature [21,22].

A recent investigation of the effects of the confinement potential and growth-direction-oriented applied magnetic fields on the binding energy and PCS of a donor impurity in an InAs Pöschl-Teller (PT) QR was presented in reference [23]. The research makes use of the effective mass approximation and a variational procedure. There, the authors reported the binding energy dependencies on the height and the inner and outer radii of the QR, the applied magnetic field, and the parameters of the PT confinement potential. Given its relevance as a precedent to the present work we should describe here the main results obtained therein: (1) the binding energy is an increasing (decreasing) function of the inner (outer) radius, (2) the binding energy is a decreasing function of the height of the QR, (3) for impurities located at the centre of the QR, the binding energy is a decreasing function of the applied magnetic field and (4) for on-centre impurities, the binding energy is a decreasing function of the asymmetry parameters of the PT.

In the case of the PCS, the results of reference [23] show that with increasing inner (outer) radius of the QR there is a blue shift (red shift) of the maximum of the lineshape of the PCS as a function of the incident photon energy.

In the present work, we extend the research described above in order to perform a predictive study of the effects of the hydrostatic pressure, applied electric and magnetic fields and impurity position on the donor binding energy and PCS in an InAs PT QR. The paper is organised as follows. In Section 2 we describe the theoretical framework. Section 3 is dedicated to the results and discussion and our conclusions are given in Section 4.

2 Theoretical framework

Figure 1 presents a pictorial view of the QR geometry considered. Specifically, we highlight the dimensions of the heterostructure (inner and outer radii and height) and the direction of the applied electric and magnetic fields.

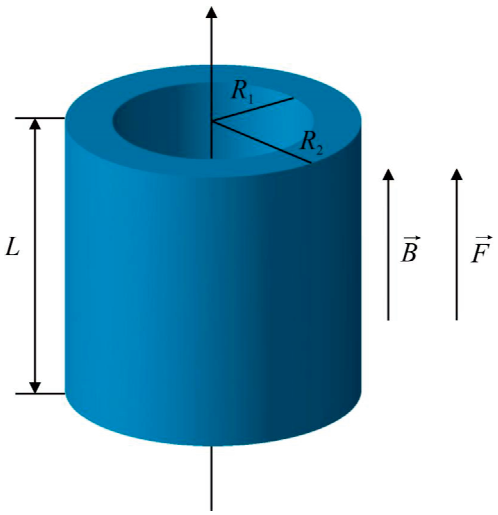

Fig. 1. (Color online) Pictorial view of the quantum ring considered in the present work.

The Hamiltonian for a hydrogenic donor impurity in an InAs QR under the influence of growth-direction applied electric and magnetic fields ($\vec{F} = F\,\hat{z}$, $\vec{B} = B\,\hat{z}$), in the effective-mass approximation, is:

$$H = \frac{1}{2\,m^*(P)}\left(\vec{p}+\frac{|e|\,\vec{A}}{c}\right)^2 + V(\rho,z,P) + |e|\,F\,z - \frac{e^2}{\varepsilon(P)\,r}, \tag{1}$$

where $r = [(\vec{\rho}-\vec{\rho_i})^2 + (z-z_i)^2]^{\frac{1}{2}}$ is the distance from the electron to the impurity site (with $(z_i,\vec{\rho_i})$ and $(z,\vec{\rho})$ being the impurity and electron coordinates, respectively), $\vec{A}$ is the vector potential, and $|e|$ is the absolute value of the electron charge. Additionally, $m^*(P)$ and $\varepsilon(P)$ are, respectively, the hydrostatic pressure dependent electron effective mass and the static dielectric constant. $V(\rho,z,P) = V_{PT}(z,P) + V(\rho,P)$ is the confinement potential of the QR, given by:

$$V(\rho,P) = \begin{cases} 0, & \text{if} \quad R_1(P) \le \rho \le R_2(P), \\ \infty, & \text{if} \quad \rho < R_1(P),\ \rho > R_2(P), \end{cases} \tag{2}$$

and:

$$V_{PT}(z,P) = \frac{\hbar^2\,\beta^2}{2\,m^*(P)}\left[\frac{\chi\,(\chi-1)}{\sin^2(\beta\,z)} + \frac{\lambda\,(\lambda-1)}{\cos^2(\beta\,z)}\right]. \tag{3}$$

The shape and symmetry of the PT potential, $V_{PT}(z,P)$, can be tuned by the values taken for the parameters χ and λ. It is perfectly symmetric when $\chi = \lambda$. Besides, as can be observed from equation (3), it has two singularities: one at $z = 0$ and the second at $z = \pi/(2\,\beta)$, where $\beta = \pi/(2\,L)$ [24].

Considering the so-called Gauge of Landau ($\vec{A} = \frac{1}{2}\,\vec{B}\times\vec{r}$), the Hamiltonian in equation (1), in cylindrical

coordinates, takes the form:

$$H = -\frac{\hbar^2}{2\,m^*(P)}\left[\frac{1}{\rho}\frac{\partial}{\partial\rho}\left(\rho\frac{\partial}{\partial\rho}\right)+\frac{1}{\rho^2}\frac{\partial^2}{\partial\phi^2}+\frac{\partial^2}{\partial z^2}\right] + \frac{i\,\hbar\,|e|\,B}{2\,m^*(P)}\frac{\partial}{\partial\phi}+\frac{m^*(P)\,\omega_H^2\,\rho^2}{8}+V(\rho,z,P) + |e|\,F\,z-\frac{e^2}{\varepsilon(P)\,r}, \quad (4)$$

where $\omega_H = \frac{|e|\,B}{m^*(P)} = \frac{\hbar}{m^*(P)\,a_H^2}$. Here a_H is the magnetic length and ω_H the cyclotron frequency.

According to the variational method, the ground-state wave function associated with the z-dependent part of the Hamiltonian in equation (4) without the impurity potential term can be expressed by [25,26]:

$$f_F(z) = N_F\,f(z)\,e^{-\alpha_F\,z} \quad (5)$$

where N_F and α_F are the normalisation constant and the electric-field-dependent variational parameter, respectively. Here, $f(z)$ is the ground-state wave function associated with the z-dependent part of the Hamiltonian in equation (4), without the impurity potential and the applied electric field terms. It is given by:

$$f(z) = \sin^{\chi}(\beta\,z)\,\cos^{\lambda}(\beta\,z). \quad (6)$$

The eigenvalue corresponding to the wave function in equation (6) is given by [27]:

$$E_z = \frac{\hbar^2\,\beta^2}{2\,m^*(P)}(\chi+\lambda)^2. \quad (7)$$

After the minimisation process, we shall call α_{F0} and E_{zF0}, respectively, the optimal values of the variational parameter and the ground-state energy along the z-direction with the applied electric field.

Because in the present work we are strictly interested in the ground state of the confined electron, we take $l = 0$ for the orbital angular momentum quantum number. Consequently, the ground-state wave function, $\vartheta(\rho)$, associated with the ρ-dependent terms of the Hamiltonian in equation (4) without the impurity potential has the following form:

$$\vartheta(\rho) = e^{-\rho^2/\left(4a_H^2\right)}\left[F\left(-\Delta,1,\frac{\rho^2}{2\,a_H^2}\right) + G_1\,U\left(-\Delta,1,\frac{\rho^2}{2\,a_H^2}\right)\right], \quad (8)$$

where F and U are the degenerate hypergeometric functions and $\Delta = \frac{m^*(P)\,E_\rho\,a_H^2}{\hbar^2} - \frac{1}{2}$ (E_ρ is the ground-state energy associated with the lateral confinement). For fixed values of R_1 and R_2, the values of E_ρ and the constant G_1 are obtained from the vanishing condition on the radial solution at the potential barriers, i.e., $\vartheta(R_1) = \vartheta(R_2) = 0$.

Following the usual variational procedure, we obtain the impurity ground-state energy by minimising the functional:

$$E_{\alpha_i} = \left.\frac{\langle\Psi_i(\rho,z)|\,H\,|\Psi_i(\rho,z)\rangle}{\langle\Psi_i(\rho,z)|\Psi_i(\rho,z)\rangle}\right|_{\min\alpha_i} \quad (9)$$

where:

$$\Psi_i(\rho,z) = f_F(z)\,\vartheta(\rho)\,e^{-\alpha_i\,r} \quad (10)$$

and α_i is the variational parameter. The impurity binding energy is defined as:

$$E_b = E_\rho + E_{zF0} - E_{\alpha_{i0}}, \quad (11)$$

where α_{i0} is the optimal value of the variational parameter.

The inclusion of hydrostatic pressure effects is made via the pressure dependence on the electron effective mass, on the InAs static dielectric constant, and on the dimensions (inner and outer radii and height of the heterostructure). They are, respectively [28,29]:

$$\frac{m^*(P)}{m_0} = \left[1+\Pi_0\left(\frac{3\,E_g(P)+2\,\Delta}{3\,E_g(P)\,(\,E_g(P)+\Delta)}\right)\right]^{-1}, \quad (12)$$

$$\varepsilon(P) = \left(12.3 - 3.2761\times10^{-2}P\right)\left(\frac{237.94+0.407P}{218.74+0.406P}\right)^2, \quad (13)$$

$$L(P) = L(0)\left[1-P\,(S_{11}+2S_{12})\right], \quad (14)$$

and

$$R_i(P) = R_i(0)\left[1-2P\,(S_{11}+2S_{12})\right]^{1/2}, \quad (i=1,2), \quad (15)$$

where m_0 is the free electron mass and $E_g(P)$ is the pressure dependent InAs band gap, which is given by:

$$E_g(P) = (532.949+\alpha P)\ \text{meV}. \quad (16)$$

In the calculations we take $\Pi_0 = 38$ eV, $\Delta = 0.38$ eV, $\alpha = 7.7$ meV/kbar, $S_{11} = 1.946\times10^{-3}$ kbar^{-1}, and $S_{12} = -6.855\times10^{-4}$ kbar^{-1} [30,31].

One may write the PCS describing the transitions from the impurity ground-state $|\Psi_i\rangle$ to the final state $|\Psi_f\rangle$ within the dipole approximation. The corresponding expression is [17,19,20,32–34]:

$$\sigma(\omega) = \frac{4\,\pi^2\,\alpha_{FS}\,\hbar\,\omega}{\varepsilon(P)^{1/2}}\left(\frac{F_{\mathit{eff}}}{F_0}\right)^2\left(\frac{m^*(P)}{m_0}\right)^2 \times\sum_f\left|\left\langle\Psi_i\left|\vec{\xi}\cdot\vec{r}\right|\Psi_f\right\rangle\right|^2\delta\left(E_f-E_i-\hbar\,\omega\right), \quad (17)$$

where α_{FS} is the fine structure constant, $\hbar\,\omega$ is the photon energy, F_{eff} is the effective electric field on the impurity, F_0 is the average field, $\vec{\xi}$ is the light wave polarization vector, and E_f and E_i are the energies of the final and initial states, respectively. The final state wave function is the eigenfunction of the Hamiltonian in equation (1) without the impurity potential term and is given by:

$$\Psi_f(\rho,z) = N_f\,\vartheta(\rho)\,f_F(z), \quad (18)$$

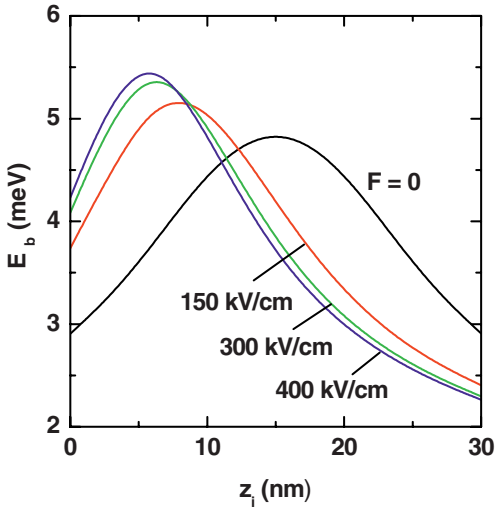

Fig. 2. (Color online) Binding energy of a donor impurity in an InAs Pöschl-Teller QR as a function of the impurity position along the z-direction. Several values of the electric field have been considered for $\chi = \lambda = 1.001$, $B = 0.1$ T, and $P = 0$.

where N_f is a normalisation constant. We have considered the case when the polarization vector is directed along the z-axis (parallel polarization). In this case the selection rules for the matrix element of the dipole moment indicate that we must take into account the transitions from the first impurity states to the ground state of the QR. Then, the PCS for parallel polarization of the incident radiation may be written as:

$$\sigma(\omega, P) = \frac{4\,\pi\,\alpha_{FS}\,\hbar\,\omega}{\varepsilon(P)} \left(\frac{F_{eff}}{F_0}\right)^2 \left(\frac{m^*(P)}{m_0}\right)^2 |I_{fi}|^2 \times \frac{\Gamma}{\left(E_b - \hbar\omega\right)^2 + \Gamma^2}, \quad (19)$$

where Γ is the Lorentzian parameter and:

$$I_{fi} = (N_i\, N_f) \times \int_0^L \int_0^{2\pi} \int_{R_1}^{R_2} z\, e^{-\alpha\, r}\, |\vartheta(\rho)\, f_F(z)|^2\, \rho\, d\rho\, d\varphi\, dz. \quad (20)$$

To our knowledge, there are no experimental measurements on the hydrostatic dependence of the Γ Lorentzian parameter. We have therefore taken the fixed value $\Gamma = 4$ meV [35].

3 Results and discussion

For all QRs studied, we have used the following fixed values of the dimensions: the inner radius $R_1 = 10$ nm, the outer radius $R_2 = 60$ nm, and height $L = 30$ nm. Then, in Figure 2 we present our results for the binding energy of a donor impurity in an InAs PT QR as a function of the impurity position along the z-direction of the QR. The calculation considers several values of electric field for $\chi = \lambda = 1.001$, $B = 0.1$ T, $P = 0$, and $\rho_i = (R_1 + R_2)/2$. In the case of zero applied electric field ($F = 0$) –and because we have taken $\chi = \lambda$–, the binding energy curve is symmetrical with respect to $z_i = L/2 = 15$ nm, with a maximum for the impurity at the center of the QR. This happens for in this case the amplitude of the probability along the z-direction, for a non-correlated electron wave function, is also symmetrical with respect to $z = L/2 = 15$ nm. With the increase of the electric field strength, the maximum of the probability for the uncorrelated electron wave function is shifted towards the $0 < z < L/2$ region, thus breaking the even symmetry with respect to the position $z = L/2$. For impurities located within the range $0 < z_i < L/2$, the expectation value of the electron-impurity distance is then smaller than the one obtained for impurities in the region $L/2 < z_i < L$. This makes the binding energy in the first case larger than that of the second case. In this sense it is valid to say that the shape of the curve for the binding energy as a function of the impurity position exhibits the same behaviour as shown by the electron probability density as a function of the z-coordinate.

It is clear from Figure 2 that with the strengthening of the electric field, the maximum value reached by the binding energy increases. This can be explained by means of the arguments that follow: as we have already mentioned, with the increase of the electric field the electron probability shifts towards the $0 < z < L/2$ region. Hence, due to the infinite potential barrier located at $z = 0$, the increase in the electric field strength is reflected in a diminishing of the effective width of the spatial region in which the electron is confined. This is, in other words, just a reinforcement of the quantum confinement and, as a consequence, the binding energy must increase. When the impurity is placed at the region $z_i \simeq 0$, the binding energy is bigger for larger value of the electric field, and this effect is reversed when the impurity is located at $z_i \simeq L$. In the limit of very large electric fields, the expectation value of the axial distance between the electron and the impurity is approximately equal to zero for impurities located at $z_i = 0$, and equal to L, for impurities located at $z_i = L$. Notice that the electric field intensities equal to or larger than 300 kV/cm have practically saturated their effects and induce no substantial changes in the electron-impurity binding energy.

In Figure 3 we present our results for the binding energy of a donor impurity in an InAs PT QR as a function of the impurity position along the z-direction of the QR. We are now changing the PT geometry by considering several values of the χ-parameter while keeping fixed the values $\lambda = 1.001$, $B = 0.1$ T, $F = 0$, and $P = 0$. Notice that in the case of $\chi = 1.001$ the PT confinement potential is symmetrical and becomes an infinite square confinement potential. This special case was discussed above in Figure 2. As the χ-parameter increases, the amplitude of probability along the z-direction for the uncorrelated electron wave function shifts from the center of the heterostructure towards the region $L/2 < z < L$. In this case, the Coulomb electron-impurity interaction strengthens for the situation in which the impurities are located within the region $L/2 < z_i < L$, whilst it weakens for impurities in the region $0 < z_i < L/2$. For this reason, the maximum of

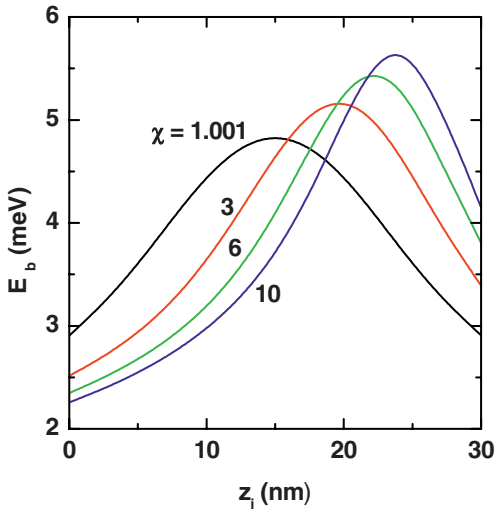

Fig. 3. (Color online) Binding energy of a donor impurity in an InAs Pöschl-Teller QR as a function of the impurity position along the z-direction. Several values of the χ-parameter of confinement potential have been considered for $\lambda = 1.001$, $B = 0.1$ T, $F = 0$, and $P = 0$.

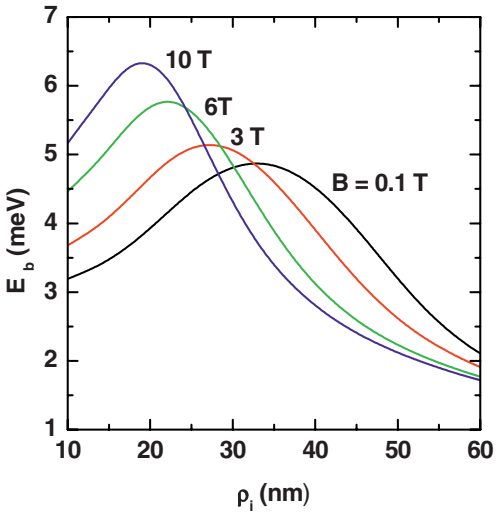

Fig. 4. (Color online) Binding energy of a donor impurity in an InAs Pöschl-Teller QR as a function of the radial impurity position. Several values of the magnetic field induction have been considered for $\chi = \lambda = 1.001$, $F = 0$, and $P = 0$.

the binding energy appears shifted to the right-hand side. This can be rationalised as an effect analogous to the one exerted by a negative electric field oriented in the opposite direction to the one considered in obtaining the results of Figure 2. For $\chi > 1.001$ the effect of the confinement potential is stronger than in the symmetrical case due to the reduction in the effective height of the QR in which the electron is confined. Therefore the Coulomb interaction and, consequently, the binding energy become larger. Notice that the binding energy is much larger when the impurity is placed close to $z_i \simeq L$. In that case the impurity is placed near the region in which the electron wave function reaches its maximum; a fact that is directly related to the asymmetry induced in the potential when one makes $\chi > 1.001$.

From both Figures 2 and 3 we can see that when the position of the impurity coincides with the centre of the QR ($z_i = L/2, \rho_i = (R_1 + R_2)/2$), the binding energy is always a decreasing function of the applied electric field strength. The same happens with the variation PT confinement parameter as long as the condition $\lambda \neq \chi$ is fulfilled. This is because, in both cases, the electric field and the asymmetry induced on the PT confinement potential push the electron probability far from the impurity. On the other hand, as long as we satisfy the condition $\lambda = \chi$ for the PT parameters, the binding energy must be an increasing function of their value given that this simultaneous increase means a reduction in the quantum disk effective height.

In Figure 4 we present the binding energy of a donor impurity in an InAs PT QR as a function of the impurity position along the radial direction of the QR. Several values of the applied magnetic field induction have been considered for $\chi = \lambda = 1.001$, $F = 0$, and $P = 0$. From the depicted results it is clear that with the increase of the magnetic field the maximum value of the donor binding energy becomes shifted towards lower values of the radial coordinate. The increase in the magnetic field induction intensity makes the electron much more localised around the axis of the QR (near to the infinite barrier located at $\rho = R_1$). For this reason, the maximum of the electron-impurity binding energy curves corresponds to impurities with radial position contained in the region $R_1 < \rho_i < (R_1 + R_2)/2$. Also we can see that in this case, when the impurity is placed at $\rho_i = R_1$, increasing the magnetic field induction causes the binding energy to rise as well. When one increases the magnetic field the maximum of the electron probability density concentrates largely within the region in which the impurity is located. As a consequence, the expectation value of the electron-impurity distance decreases and, in turn, the Coulomb interaction is reinforced. Notice that when the impurity is placed at $\rho_i = R_2$, the binding energy decreases with increasing magnetic field because the electron-impurity interaction weakens.

The results regarding the combined effects of the hydrostatic pressure and the impurity position on the binding energy of a donor impurity in an InAs PT-QR can be found in Figures 5a and 5b. In this case, the calculation is done taking $\chi = \lambda = 1.001$, and $F = 0$, and $B = 1$ T. It is readily seen that in all cases, the influence of the hydrostatic pressure leads to an increase in the binding energy. There are several factors which are responsible for such behaviour, namely that as long as the hydrostatic pressure increases, (1) the InAs dielectric constant diminishes, (2) the electron effective mass increases and (3) the dimensions of the structure decrease. With the increase of the effective mass, the first non-correlated electron confined state goes down in energy. On the other hand, the reduction of the dielectric constant leads to the weakening of the electrostatic screening with the consequent reinforcement of the Coulombic interaction and the growth of the binding energy value. Reducing the effective dimensions of the

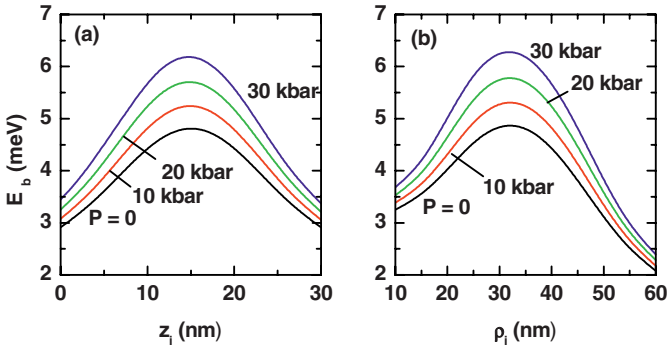

Fig. 5. (Color online) Binding energy of a donor impurity in an InAs Pöschl-Teller QR as a function of the impurity position along the z-direction (a) and along the radial direction (b) for several values of the hydrostatic pressure with $\chi = \lambda = 1.001$, $F = 0$, and $B = 1$ T.

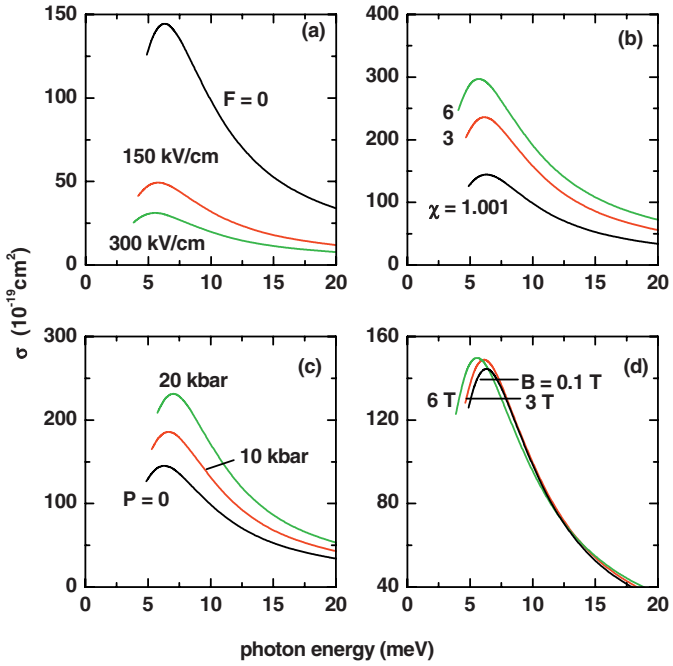

Fig. 6. (Color online) Photoionisation cross section of a donor impurity in an InAs Pöschl-Teller QR as a function of the photon energy for parallel polarisation of the incident radiation. Several values of electric field (with $\chi = \lambda = 1.001$, $B = 0.1$ T, $P = 0$) (a); χ-parameter (with $\lambda = 1.001$, $F = 0$, $B = 0.1$ T, $P = 0$) (b); hydrostatic pressure (with $\chi = \lambda = 1.001$, $F = 0$, $B = 1$ T) (c), and magnetic field induction (with $\chi = \lambda = 1.001$, $F = 0$, $P = 0$) (d) have been considered.

structure results in shortening of the effective electron-impurity distance, which also leads to an increase in E_b. As can be seen from the figures, the influence of the hydrostatic pressure does not modify the overall phenomenology associated with the binding energy curves.

In Figure 6 we present the PCS of a donor impurity in an InAs PT-QR as a function of the incident photon energy in the case of parallel polarization of the incident radiation. The impurity is placed on the centre of the QR ($z_i = L/2, \rho_i = (R_1 + R_2)/2$). Our calculation includes

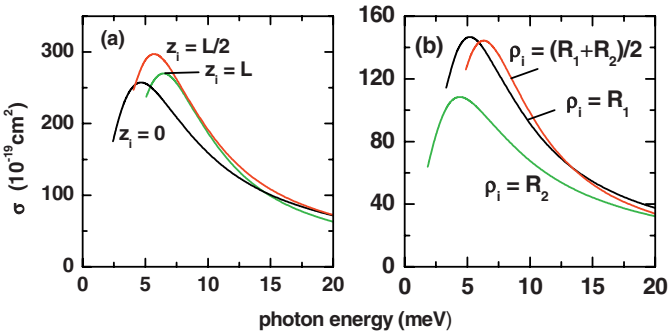

Fig. 7. (Color online) Photo-ionization cross section of a donor impurity in an InAs Pöschl-Teller QR as a function of the photon energy for parallel polarization of the incident radiation. Several values of the impurity position along the z-direction (a) and radial direction (b) have been considered for $\lambda = 1.001$, $F = 0$, and $B = 0.1$ T. In (a) results are for $\chi = 6$ with $\rho_i = (R_1 + R_2)/2$ whereas in (b) the results are for $\chi = 1.001$ with $z_i = L/2$.

several values of the electric field (a), PT χ-parameter (b), hydrostatic pressure (c) and magnetic field induction (d). From Figure 6 it is clear that in all cases the PCS has a threshold behaviour. Figures 6a, 6b and 6d show that with the respective increase of the electric field, the χ-parameter and the magnetic field induction, the threshold energy of the PCS decreases. The explanation of this fact lies in the decrease of the on-centre donor binding energy (see Figs. 2–4 respectively). Also Figure 6c shows that with the increase of the hydrostatic pressure the threshold energy of the PCS increases, which is a consequence of the increase of the binding energy (see Fig. 5). So, the results show that the decrease (increase) of the binding energy associated either with the electric field, the magnetic field, and the parameter of the PT-confinement potential (hydrostatic pressure) leads to the red shift (blue shift) of the maximum of the PCS spectrum. Notice that the shape of the PCS does not depend on the light polarization, because in analogy to the case of a QD, in the QR the electron is also confined in all directions of the space. But there are different selection rules: in the case of a cylindrical QD when the polarization vector is directed along the radial direction of the QD for an on-centre impurity ($z_i = 0, \rho_i = 0$) the transition from the ground impurity state to the ground state of the cylindrical QD is forbidden [16]. However, in the case of a QR the impurity is always found at $\rho_i \neq 0$ and the mentioned transitions are allowed.

Figure 7 contains our results for the PCS of a donor impurity in an InAs PT-QR as a function of the incident photon energy in the situation of parallel polarization of the incident radiation. In this case, the parameters chosen to vary are both the axial and radial impurity positions. In Figure 7a, taking into account an asymmetrical potential configuration, it is clearly observed that when the impurity is placed at $z_i = 0$ and $z_i = L$ there will be distinct PCS threshold energies due to the asymmetry induced by the difference between the two PT-potential parameters. This is reflected in different values of E_b for an impurity

localised at a given position and, at the same time, manifests through a variety of minimum-photon-energy values capable of generating transitions, as is readily seen in the figure. Figure 7b shows that for the chosen value of the magnetic field, the threshold energy of the PCS is a maximum when the impurity is placed on the centre of the QR, which coincides with the result shown in Figure 4. Also, we can see that when the radial impurity position is $\rho_i = R_1$ the threshold energy is bigger than when the impurity is placed on $\rho_i = R_2$. This fact can also be explained by observing the corresponding behaviour of the binding energy reported in Figure 4b.

4 Conclusions

In this article we have studied the combined influence of hydrostatic pressure, electric and magnetic fields, and impurity position on donor binding energy and photo-ionization cross section in an InAs quantum ring with Pöshl-Teller confinement potential along the axial direction. Our results show that the impurity position along the growth and radial directions can significantly modify the influence of external electric and magnetic fields, and the influence of the asymmetry degree of the Pöschl-Teller confinement potential on the donor impurity binding energy. Also, we have shown that the binding energy is an increasing function of hydrostatic pressure. Additionally, we have found that the decrease (increase) of the binding energy with the electric and magnetic fields and the parameters of confinement potential (hydrostatic pressure) leads to a red shift (blue shift) of the maximum of the photo-ionization cross section of an on-centre impurity.

CAD and MEMR thank CONACYT (Mexico) and COLCIENCIAS (Colombia) for support under the 2009-2011 Bilateral Agreement "*Estudio de los efectos de la presión hidrostática y la mezcla de estados de conducción sobre la estructura electrónica y los estados excitónicos en nanoestructuras basadas en semiconductores III-V*". MEMR also acknowledges support from Mexican CONACYT through grant CB-2008-101777. CAD is grateful to the Colombian Agencies CODI-Universidad de Antioquia (Estrategia de Sostenibilidad Grupo de Materia Condensada-UdeA, 2011-2012), Facultad de Ciencias Exactas y Naturales-Universidad de Antioquia (CAD-exclusive dedication project 2011-2012), and "El Patrimonio Autónomo Fondo Nacional de Financiamiento para la Ciencia, la Tecnología y la Innovación Francisco José de Caldas" Contract RC No. 275-2011. The work was developed with the help of CENAPAD-SP, Brazil. This work was partially financed by the Armenian State Committee of Science (Project No. 11B-1c039).

References

1. P.M. Petroff, A. Lorker, A. Imamoglu, Phys. Today, 46 (2001)
2. D. Bimberg, M. Grundman, N.N. Ledentsov, *Quantum Dot Heterostructures* (John Wiley Sons, Chichester, 1999)
3. O. Benson, C. Santori, M. Pelton, Y. Yamamoto, Phys. Rev. Lett. **84**, 2513 (2000)
4. F. Suárez, D. Granados, M.L. Dotor, M.G. García, Nanotechnology **15**, S126 (2004)
5. H.S. Ling, S.Y. Wang, C.P. Lee, M.C. Lo, J. Appl. Phys. **105**, 034504-1 (2009)
6. F. Troiani, U. Hohenester, E. Molinari, Phys. Rev. B **62**, R2263 (2000)
7. W.E. Kerr, A. Pancholi, V.G. Stoleru, Physica E **35**, 139 (2006)
8. A. Lorke, R.J. Luyken, A.O. Govorov, J.P. Kotthaus, J.M. Garcia, P.M. Petroff, Phys. Rev. Lett. **84**, 2223 (2000)
9. A.D. Yoffe, Adv. Phys. **50**, 1 (2001)
10. Z. Barticevic, M. Pacheco, A. Latgé, Phys. Rev. B **62**, 6963 (2000)
11. A. Bruno-Alfonso, A. Latgé, Phys. Rev. B **61**, 15887 (2000)
12. B.S. Monozon, P. Schmelcher, Phys. Rev. B **67**, 045203 (2003)
13. M. Aichinger, S.A. Chin, E. Krotscheck, E. Räsänen, Phys. Rev. B **73**, 195310 (2006)
14. M. Takikawa, K. Kelting, G. Brunthaler, M. Takeshi, J. Komena, J. Appl. Phys. **65**, 3937 (1989)
15. M. El-Said, M. Tomak, Solid State Commun. **82**, 721 (1992)
16. M.G. Barseghyan, A.A. Kirakosyan, C.A. Duque, Eur. Phys. J. B **72**, 521 (2009)
17. A. Sali, M. Fliyou, H. Satori, H. Loumrhari, J. Phys. Chem. Solids **64**, 31 (2003)
18. E. Kasapoglu, U. Yesilgül, H. Sari, I. Sökmen, Physica B **368**, 76 (2005)
19. V.N. Mughnetsyan, M.G. Barseghyan, A.A. Kirakosyan, Physica E **40**, 654 (2008)
20. V.N. Mughnetsyan, M.G. Barseghyan, A.A. Kirakosyan, Superlattices Microstruct. **44**, 86 (2008)
21. J.D. Correa, N. Porras-Montenegro, C.A. Duque, Phys. Stat. Sol. B **241**, 2440 (2004)
22. M.G. Barseghyan, A. Hakimyfard, S.Y. López, C.A. Duque, A.A. Kirakosyan, Physica E **42**, 1618 (2010)
23. M.G. Barseghyan, A. Hakimyfarda, M. Zuhair, C.A. Duque, A.A. Kirakosyan, Proc. SPIE **7998**, 79981G (2010)
24. S. Flugge, *Practical Quantum Mechanics I* (Springer-Verlag, Berlin, Heidelberg, 1971)
25. G. Bastard, E.E. Mendez, L.L. Chang, L. Esaki, Phys. Rev. B **28**, 3241 (1983)
26. M.G. Barseghyan, A. Hakimyfard, S.Y. López, C.A. Duque, A.A. Kirakosyan, Physica E **43**, 529 (2010)
27. H. Yildirim, M. Tomak, Eur. Phys. J. B **50**, 559 (2006)
28. A.H. Rodríguez, C. Trallero-Ginner, C.A. Duque, G.J. Vázquez, J. Appl. Phys. **105**, 044308 (2009)
29. S.Q. Wang, H.Q. Ye, J. Phys.: Condens. Matter **17**, 4475 (2005)
30. P.Y. Yu, M. Cardona, *Fundamentals of Semiconductors* (Springer-Verlag, Berlin, 1996)
31. C. Trallero-Giner, A. Alexandrou, M. Cardona, Phys. Rev. B **38**, 10744 (1988)
32. G. Lamouche, Y. Lepin, Phys. Rev. B **49**, 13452 (1994)
33. H. Ham, H.N. Spector, J. Appl. Phys. **93**, 3900 (2003)
34. M. Sahin, Phys. Rev. B **77**, 045317 (2008)
35. P.K. Basu, *Theory of Optical Processes in Semiconductors* (Clarendon Press, Oxford, 1997)